Available online at www.sciencedirect.com

ScienceDirect

International Journal of Solids and Structures 43 (2006) 6071–6084

INTERNATIONAL JOURNAL OF SOLIDS and STRUCTURES

www.elsevier.com/locate/ijsolstr

Scale effect on wave propagation of double-walled carbon nanotubes

Q. Wang [a,*], G.Y. Zhou [b], K.C. Lin [b]

[a] *Department of Mechanical and Manufacturing Engineering, University of Manitoba, Winnipeg, MB R3T 2N2, Canada*
[b] *Department of Mechanical, Materials and Aerospace Engineering, University of Central Florida, Orlando, FL 32816-2450, USA*

Received 22 May 2005; received in revised form 16 November 2005
Available online 25 January 2006

Abstract

Scale effect on transverse wave propagation in double-walled carbon nanotubes (DWNTs) is studied via nonlocal elastic continuous models. The nonlocal Euler–Bernoulli and Timoshenko beam models are proposed to study the small-scale effect on wave dispersion results for DWNTs with respect to the variation of DWNT's wavenumbers and diameters by theoretical analyses and numerical simulations. The cut-off frequency, asymptotic phase velocity, and asymptotic frequency are also derived from the nonlocal continuum models. A rough estimation on the scale coefficient used in the nonlocal continuum models is proposed for the study of carbon nanotubes (CNTs) in the manuscript. The diameter-dependent dispersion relations for DWNTs via the nonlocal continuum models are observed as well. In addition, the applicability of the two beam models is explored by numerical simulations. The research work reveals the significance of the small-scale effect on wave propagation in multi-walled carbon nanotubes.

Keywords: Carbon nanotubes; Wave propagation; Nonlocal continuum mechanics; Euler–Bernoulli beam; Timoshenko beam; Cut-off frequency; Asymptotic velocity; Dispersion relations

1. Introduction

Carbon nanotubes (CNTs) have become one of the most promising new materials for nanotechnology (Ball, 2001; Baughman et al., 2002; Ajayan and Zhou, 2001) due to their novel electronic and mechanical properties. Some of the examples of CNTs applications are atomic-force microscope, field emitters, nano-fillers for composite materials, nanoscale electronic devices, and even frictionless nano-actuators, nano-motors, nano-bearings, and nano-springs (Lau, 2003). The modeling for CNTs is classified into two main categories. The first one is the atomic modeling, including the techniques such as classical molecular dynamics, tight binding molecular dynamics and density functional model (Iijima et al., 1996; Yakobson et al., 1997; Hernandez et al., 1998; Sanchez-Portal et al., 1999). These atomic methods are only limited to systems with a small

* Corresponding author. Tel.: +1 407 8235828; fax: +1 407 8230208.
E-mail address: qzwang@mail.ucf.edu (Q. Wang).

0020-7683/$ - see front matter © 2005 Elsevier Ltd. All rights reserved.
doi:10.1016/j.ijsolstr.2005.11.005

number of molecules and atoms and therefore only restrained to the study of small-scale modeling. Unlike classical molecular dynamics, continuum model is practical in analyzing CNTs for large-scale systems. Yakobson et al. (1996) studied the unique features of fullernes and developed a continuum shell model in studying different instability patterns of a CNT under different compressive load. Ru (2000b) proposed the buckling analysis of CNTs with shell models. Krishnan et al. (1998) estimated Young's modulus of singled-walled carbon nanotubes (SWNTs) by observing their freestanding room-temperature vibrations in a transmission electron microscope. Wang (2004) proposed the effective in-plane stiffness and bending rigidity of armchair and zigzag CNTs through the analysis of a representative volume element of the graphene layer via continuous elastic models. Wang et al. (2005) studied the bending instability characteristics of DWNTs of various configurations using a hybrid approach. The research showed that the bending instability may take place through the formation of a single kink in the midpoint of a DWNT or two kinks, placed symmetrically about the midpoint, depending upon both the tube length and diameters.

The small-size scales associated nanotechnology are often sufficiently small to call the applicability of classical continuum models into question for nano-structures with very small dimensions. Classical or local continuum models, such as beam and shell models, do not admit intrinsic size dependence in the elastic solutions of inclusions and inhomogeneities. At nanometer scales, however, size effects often become prominent, the cause of which need to be explicitly addressed with an increasing interest in the general area of nanotechnology (Sharma et al., 2003). The modeling of such a size-dependent phenomenon has become an interesting subject of some researches in this field (Sheehan and Lieber, 1996; Yakobson and Smalley, 1997). It is thus concluded that the applicability of classical continuum models at very small scales is questionable, since the material microstructure at small size, such as lattice spacing between individual atoms, becomes increasingly important and the discrete structure of the material can no longer be homogenized into a continuum. Therefore, newly proposed continuum model rather than the classical continuum models may be an alternative to take into account the scale effect in the studies of nanomaterials.

The scale effect was accounted for in elasticity by assuming the stress at a reference point is considered to be a functional of the strain field at every point in the body by theory of NONLOCAL elasticity (Eringen, 1976). In this way, the internal size scale could be considered in the constitutive equations simply as a material parameter. The application of nonlocal elasticity models in nanomaterials was proposed by Peddieson et al. (2003). They applied the nonlocal elasticity to formulate a nonlocal version of Euler–Bernoulli beam model, and concluded that nonlocal continuum mechanics could potentially play a useful role in nanotechnology applications. Further applications of the nonlocal continuum mechanics have been employed in studying the mechanical behavior of CNTs. Sudak (2003) studied the infinitesimal column buckling of multi-walled nanotubes (MWNTs) incorporating not only van der Waals forces but also the effects of small length scales. His results showed that as the small length scale increases in magnitude the critical axial strain decreases compared to the results with classical continuum mechanics. Zhang et al. (2004) proposed a nonlocal multi-shell model for the axial buckling of MWNTs under axial compression. Their results showed that the influence of the small scale on the axial buckling strain is related to the buckling mode and the length of tubes.

Growing interest in terahertz physics of nanoscale materials and devices (Sirtori, 2002; Jeon and Kim, 2002; Antonelli and Maris, 2002; Brauns et al., 2002) opens a new topic on wave characteristics of CNTs, especially on the terahertz frequency range. Yoon et al. (2003, 2004) studied the wave propagation of MWNTs. In their studies, van der Waals force was modeled via their multiple-beam model. In structural analysis of one-dimensional beam-like structures, two models are usually employed, namely Euler–Bernoulli and Timoshenko beam models. Both models assume that plane sections remain plane. But in Euler–Bernoulli beam model, the sections remain perpendicular to the neutral axis whereas this assumption is removed in Timoshenko beam model (1921) to account for the effect of shear and rotary effect. Euler–Bernoulli beam model normally provides over-estimated wave phase velocity at higher wavenumber. Timoshenko beam model, on the other hand, is proved to be able to provide more accurate wave solution even at higher frequency range, although it is more complicated than Euler–Bernoulli beam model. The above investigations conducted the feasibility of the two local beam models in analysis of wave propagation of CNTs on terahertz frequency range. However, the small-scale effect was never considered in the published results. Since terahertz physics of nanoscale materials and devices are the main concerns in the wave characteristic of CNTs, the small-scale effect must be obvious as the wavelength in the frequency domain is in the order of *nanometer*.

The research in this manuscript will study the scale effect on wave propagation of DWNTs via nonlocal continuum mechanics. Two nonlocal beam modes, i.e. Euler–Bernoulli and Timoshenko models, are proposed for the analysis. The wave characteristic solution is studied with respect to the wavenumbers, the scale coefficient, and diameters of DWNTs. It is hoped the research in the manuscript will provide benchmark results on nonlocal continuum mechanics in wave propagation of MWNTs.

2. Nonlocal continuum models of CNTs

In theory of nonlocal elasticity (Eringen, 1976), the stress at a reference point x is considered to be a functional of the strain filed at every point in the body. This observation is in accordance with atomic model of lattice dynamics and experimental observations on phonon dispersion.

The basic equations for linear, homogeneous, isotropic, nonlocal elastic solid with zero body force are given by

$$\sigma_{ij,j} = 0 \tag{1a}$$

$$\sigma_{ij}(x) = \int \alpha(|x - x'|, \tau) C_{ijkl} \varepsilon_{kl}(x') \mathrm{d}V(x') \quad \forall x \in V \tag{1b}$$

$$\varepsilon_{ij} = \frac{1}{2}(u_{i,j} + u_{j,i}) \tag{1c}$$

where C_{ijkl} is the elastic modulus tensor of classical isotropic elasticity; σ_{ij} and ε_{ij} are stress and strain tensors respectively, and u_i is displacement vector. $\alpha(|x - x'|, \tau)$ is the nonlocal modulus or attenuation function incorporating into the constitutive equations to characterize the nonlocal effects at the reference point x produced by local strain at the source x'. $|x - x'|$ is the Euclidean distance, and $\tau = e_0 a/l$ (Eringen, 1983), where e_0 is a constant appropriate to each material, a is an internal characteristic length (e.g. length of C–C bond, lattice parameter, granular distance), and l is an external characteristic length (e.g. crack length, wavelength). It is noted that the value of e_0 needs to be determined from experiments or by matching dispersion curves of plane waves with those of atomic lattice dynamics. In the limit when the effects of strains at points other than x is neglected, one obtains classical (local) model of elasticity by setting $e_0 = 0$.

Integral–partial differential equations of the above linear nonlocal elasticity has been proposed leading to singular partial differential equations of a special class of physically admissible kernel (Eringen, 1983). In addition, Hook's law for an unaxial stress state was determined by

$$\sigma(x) - (e_0 a)^2 \frac{\mathrm{d}^2 \sigma(x)}{\mathrm{d}x^2} = E\varepsilon(x) \tag{2}$$

where E is Young's modulus of the material. Thus, the scale coefficient $e_0 a$ in the modeling will lead to small-scale effect on the response of structures in nano-size.

To investigate the small-scale effect on the wave solutions of DWNTs, nonlocal Euler–Bernoulli and Timoshenko beam models are proposed hereinafter.

2.1. Nonlocal Euler–Bernoulli beam model

The equilibrium equations on the force in vertical direction and the moment on a free body diagram of an infinitesimal element of a beam structure shown in Fig. 1 can be easily provided below:

$$\frac{\partial V}{\partial x} - \rho A \frac{\partial^2 u}{\partial t^2} = 0 \tag{3a}$$

$$V - \frac{\partial M}{\partial x} = 0 \tag{3b}$$

where $V(x, t)$ and $M(x, t)$ are resultant shear force and bending moment on the beam; ρ is the mass density of the material, A is the cross-area, and $u(x, t)$ is the flexural deflection of the beam.

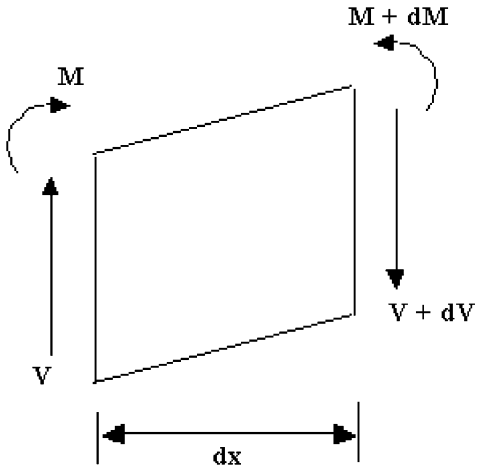

Fig. 1. Free body diagram of a beam element.

Consider definitions of the resultant bending moment and the kinematics relation in a beam structure:

$$M = \int_A y\sigma \, \mathrm{d}A \tag{4a}$$

$$\varepsilon = -y\frac{\partial^2 u}{\partial x^2} \tag{4b}$$

where y is the coordinate measured from the mid-plane in the height direction of the beam.

Substituting Eqs. (4a) and (4b) into the nonlocal constitutive relation Eq. (2) leads to

$$M - (e_0 a)^2 \frac{\partial^2 M}{\partial x^2} = -\mathrm{EI}\frac{\partial^2 u}{\partial x^2} \tag{5}$$

where EI is the bending rigidity of the beam structure. Eq. (5) will become the following expression by considering Eqs. (3a)–(4b):

$$\mathrm{EI}\frac{\partial^4 u}{\partial x^4} + \rho A \frac{\partial^2}{\partial t^2}\left(u - (e_0 a)^2 \frac{\partial^2 u}{\partial x^2}\right) = 0 \tag{6}$$

from which the local Euler–Bernoulli beam model is recovered if the scale coefficient e_0 is identically zero.

2.2. Nonlocal Timoshenko beam model

In Timoshenko beam model, a new variable φ is introduced to measure the slope of the cross-section due to bending. Now the slope of the centroidal axis, $\frac{\partial u}{\partial x}$, is made up of two contributions, i.e. φ representing the effect of bending and γ_0 representing shear effects. The essence of Timoshenko argument is that the shear force at the cross-section is given in terms of the shear strain γ as

$$V = G\int_A \gamma \, \mathrm{d}A \tag{7}$$

where $G = \frac{E}{2(1+\upsilon)}$ is the shear modulus of CNTs. If γ_0 is the shear strain at the centroidal axis, then $G\gamma_0 A$ will give a shear force. However, it will not be equal to the value given in Eq. (7). To bring the value into balance, the adjustment coefficient κ is introduced such that

$$V = G\int_A \gamma \, \mathrm{d}A = \kappa(G\gamma_0 A) = AG\kappa\left(\frac{\partial u}{\partial x} - \phi\right) \tag{8}$$

κ is the adjustment coefficient which is suggested to take as 10/9 for a circular shape of the cross-area (Timoshenko, 1921).

The motion equation of beams based on the nonlocal Timoshenko beam model can be given as follows:

$$\frac{\partial V}{\partial x} = \rho A \frac{\partial^2 u}{\partial t^2} \tag{9a}$$

$$V - \frac{\partial M}{\partial x} = \rho I \frac{\partial^2 \phi}{\partial t^2} \tag{9b}$$

where the term on the right-hand side of Eq. (9b) is the rotary effect considered in the Timoshenko beam model.

Substitution of Eqs. (5) and (8) into Eqs. (9a) and (9b) leads to the following nonlocal Timoshenko beam model:

$$GA\kappa\left(\frac{\partial \varphi}{\partial x} - \frac{\partial^2 u}{\partial x^2}\right) + \rho A \frac{\partial^2 u}{\partial t^2} = 0 \tag{10a}$$

$$GA\kappa\left(1 - (e_0 a)^2 \frac{\partial^2}{\partial x^2}\right)\left(\frac{\partial u}{\partial x} - \varphi\right) + \mathrm{EI}\frac{\partial^2 \varphi}{\partial x^2} - \rho I \frac{\partial^2}{\partial t^2}\left(\varphi - (e_0 a)^2 \frac{\partial^2 \varphi}{\partial x^2}\right) = 0 \tag{10b}$$

It is again seen that the local Timoshenko beam model is recovered when the parameter e_0 is identically zero.

3. Wave propagation of DWNTs by nonlocal continuum mechanics

In linear analysis of DWNT's wave propagation, the van der Waals interaction pressure at any point between two adjacent tubes was modeled by a linear function of the deflection jump at that point (Yoon et al., 2004). In terms of the above model of the van der Waals interaction, the governing equations for the inner and outer tubes can be proposed accordingly. The solution for wave propagation of CNTs will thus be derived via the nonlocal Euler–Bernoulli and Timoshenko beam models hereinafter.

3.1. Nonlocal Euler–Bernoulli beam model

The governing equation for DWNT's wave propagation by considering van der Waals effect via nonlocal continuum mechanics provided in Eq. (6) is given as:

$$\mathrm{EI}_1 \frac{\partial^4 u_1}{\partial x^4} + \rho A_1 \frac{\partial^2}{\partial t^2}\left(u_1 - (e_0 a)^2 \frac{\partial^2 u_1}{\partial x^2}\right) = c(u_2 - u_1) \tag{11a}$$

$$\mathrm{EI}_2 \frac{\partial^4 u_2}{\partial x^4} + \rho A_2 \frac{\partial^2}{\partial t^2}\left(u_2 - (e_0 a)^2 \frac{\partial^2 u_2}{\partial x^2}\right) = c(u_1 - u_2) \tag{11b}$$

where EI_i, $i = 1, 2$, stand for the bending rigidities of the inner and outer tubes, $u_1(x, t)$ and $u_2(x, t)$ the bending deflections of the inner and outer tubes, A_i, $i = 1, 2$, the cross-area of the tubes, $c = Cd$ and $C = 1.0 \times 10^{20}$ J/m^4 the energy constant, $d = (d_1 + d_2)/2$ the average diameter. The coefficient C is actually a curvature-related variable in CNT analysis (Wang et al., 2005). However, in the manuscript, it is assumed to be a constant and the van der Waals force is given on the right-hand sides of Eqs. (11a) and (11b).

The wave propagation solution for Eqs. (11a) and (11b) can be expressed as follows:

$$u_i(x, t) = U_i e^{\mathrm{i}(kx - \omega t)}, \quad i = 1, 2 \tag{12a, b}$$

where U_i is the amplitude of the wave motion, k is the wavenumber, and ω is the frequency of the wave motion.

Substitution of Eqs. (12a,b) into Eqs. (11a) and (11b) yields the following equation in matrix form:

$$\begin{bmatrix} \mathrm{EI}_1 k^4 - \rho A_1 \omega^2 (1 + (e_0 a)^2 k^2) + c & -c \\ -c & \mathrm{EI}_2 k^4 - \rho A_2 \omega^2 (1 + (e_0 a)^2 k^2) + c \end{bmatrix} \begin{Bmatrix} U_1 \\ U_2 \end{Bmatrix} = \begin{Bmatrix} 0 \\ 0 \end{Bmatrix} \tag{13}$$

from which the wave solution can be derived from an eigen-value problem for non-trivial solution of U_i $(i = 1, 2)$ as follows:

$$\det\begin{bmatrix} \mathrm{EI}_1 k^4 - \rho A_1 \omega^2 (1 + (e_0 a)^2 k^2) + c & -c \\ -c & \mathrm{EI}_2 k^4 - \rho A_2 \omega^2 (1 + (e_0 a)^2 k^2) + c \end{bmatrix} = 0 \tag{14}$$

where det(·) stands for determinant of a matrix.

The two-mode phase velocity, $v = \omega/k$, for the DWNT can thus be explicitly determined from Eq. (14) as

$$v_1 = \left(\frac{P - \sqrt{P^2 - 4QR}}{2} \right)^{1/2} \tag{15a}$$

$$v_2 = \left(\frac{P + \sqrt{P^2 - 4QR}}{2} \right)^{1/2} \tag{15b}$$

where $P = \rho A_1 (1 + (e_0 a)^2 k^2) \mathrm{EI}_1 k^2 + \rho A_2 (1 + (e_0 a)^2 k^2) \mathrm{EI}_2 k^2 + \frac{c}{k^2} (\rho A_1 (1 + (e_0 a)^2 k^2) + \rho A_1 (1 + (e_0 a)^2 k^2))$, $Q = \rho A_1 (1 + (e_0 a)^2 k^2) * \rho A_1 (1 + (e_0 a)^2 k^2)$, $R = c(\mathrm{EI}_1 + \mathrm{EI}_2) + \mathrm{EI}_1 * \mathrm{EI}_2 k^4$.

The cut-off frequency derived for the DWNT by both local and nonlocal Euler–Bernoulli beam models is thus derived as

$$\omega_c^2 = c \left(\frac{1}{\rho A_1} + \frac{1}{\rho A_2} \right) \tag{16}$$

Two asymptotic phase velocities can be determined as well from Eqs. (15a) and (15b) as follows:

$$v_{a1} = \frac{1}{e_0 a} \sqrt{\frac{\mathrm{EI}_1}{\rho A_1}} \tag{17a}$$

$$v_{a2} = \frac{1}{e_0 a} \sqrt{\frac{\mathrm{EI}_2}{\rho A_2}} \tag{17b}$$

As is known, appropriate expressions of mechanical and material properties are critical in determining accurate solutions. Ru (2000a) proposed that the effective bending rigidity of a SWNT should be regarded as an independent material parameter not related to the equilibrium thickness by the elastic bending stiffness formula. Actually in all the lower-order models for beams, plates and shells, the common assumption used is the "straight normal postulate" which states that the longitudinal deformation at any point in the flexural direction is proportional to the distance between this point to the mid-plane of mid-surface of the structure. However, the atomic layer in a SWNT cannot be divided into different layers and the flexural strain or deformation are actually concentrated on a narrow region around the center-line of the atom layer, rather than distributed linearly over the thickness direction (Ru, 2000a). Based on the above discussion, the expressions for mechanical and material properties of both SWNTs and DWNTs were proposed in a reference (Wang and Varadan, 2005) which will be adopted in the current research.

The dispersion curves for two modes of the transverse wave propagation of the DWNT with the mid-surface diameter $d = 5$ nm are plotted in Fig. 2 at $e_0 a = 0$ nm, 1 nm, 2 nm respectively to study the scale effect. As is seen from the figure that the two-mode phase velocities from the local or classical Euler–Bernoulli beam model, i.e. $e_0 a = 0$ nm, show a virtual linear variation at large wavenumbers, whereas, the velocities from the nonlocal model have their asymptotic values as given in Eqs. (17a) and (17b). On the other hand, the derived phase velocities decrease with increase of the scale coefficient $e_0 a$. The difference of the phase velocities becomes more obvious at larger wavenumbers, although this difference is almost invisible at very small wavenumbers, e.g. $k < 2 \times 10^8$/m, from the simulations in Fig. 2. From the simulations, the scale effect on dispersive solution of DWNT via nonlocal Euler–Bernoulli beam model is clearly observed.

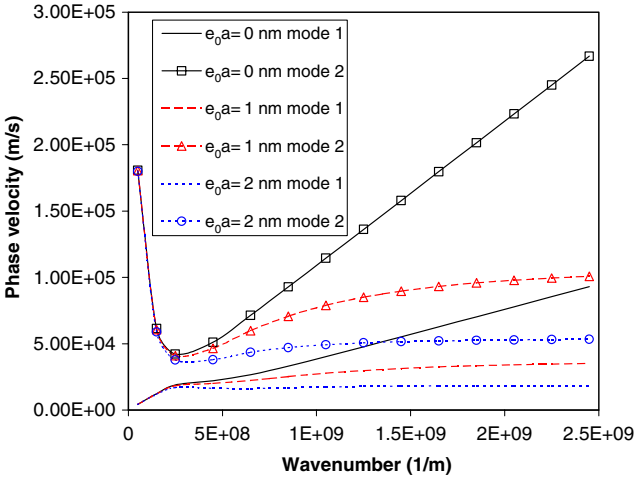

Fig. 2. Dispersive curves from Euler–Bernoulli beam models.

Since, in Timoshenko beam model, effect of shear and rotary inertia is accounted, it was concluded by Timoshenko (1921) that the wave propagation solution by this model is in better agreement with those using exact theory. Next, the scale effect on DWNT's wave solution is examined via the nonlocal Timoshenko beam model.

3.2. Nonlocal Timoshenko beam model

The governing equation for DWNT's wave propagation by considering van der Waals effect via the nonlocal Timoshenko beam model provided in Eqs. (10a) and (10b) is given as

$$GA_1\kappa\left(\frac{\partial\varphi_1}{\partial x}-\frac{\partial^2 u_1}{\partial x^2}\right)+\rho A_1\frac{\partial^2 u_1}{\partial t^2}=c(u_2-u_1) \tag{18a}$$

$$GA_1\kappa\left(1-(e_0a)^2\frac{\partial^2}{\partial x^2}\right)\left(\frac{\partial u_1}{\partial x}-\varphi_1\right)+\mathrm{EI}_1\frac{\partial^2\varphi_1}{\partial x^2}-\rho I_1\frac{\partial^2}{\partial t^2}\left(\varphi_1-(e_0a)^2\frac{\partial^2\varphi_1}{\partial x^2}\right)=0 \tag{18b}$$

$$GA_2\kappa\left(\frac{\partial\varphi_2}{\partial x}-\frac{\partial^2 u_2}{\partial x^2}\right)+\rho A_2\frac{\partial^2 u_2}{\partial t^2}=c(u_1-u_2) \tag{19a}$$

$$GA_2\kappa\left(1-(e_0a)^2\frac{\partial^2}{\partial x^2}\right)\left(\frac{\partial u_2}{\partial x}-\varphi_2\right)+\mathrm{EI}_2\frac{\partial^2\varphi_2}{\partial x^2}-\rho I_2\frac{\partial^2}{\partial t^2}\left(\varphi_2-(e_0a)^2\frac{\partial^2\varphi_2}{\partial x^2}\right)=0 \tag{19b}$$

Similarly, the subscript i ($i=1, 2$) indicates the variables on inner and outer tubes separately.

The above four equations can be reduced to two equations about $u_1(x, t)$ and $u_2(x, t)$ as follows through careful differential operations which are omitted in the current manuscript:

$$\begin{aligned}&\frac{\mathrm{EI}_1}{\rho A_1}\frac{\partial^4 u_1}{\partial x^4}-\frac{I_1}{A_1}\left(1+\frac{E}{G\kappa}\right)\frac{\partial^4 u_1}{\partial x^2\partial t^2}+\frac{\partial^2 u_1}{\partial x^2}+\frac{\rho I_1}{GA_1\kappa}\frac{\partial^4 u_1}{\partial t^4}\\&+\frac{c}{GA_1\kappa}\left(-\frac{GA_1\kappa}{\rho A_1}(u_2-u_1)+\frac{\mathrm{EI}_1}{\rho A_1}\left(\frac{\partial^2 u_2}{\partial x^2}-\frac{\partial^2 u_1}{\partial x^2}\right)-\frac{\rho I_1}{\rho A_1}\left(\frac{\partial^2 u_2}{\partial t^2}-\frac{\partial^2 u_1}{\partial t^2}\right)\right)\\&+(e_0a)^2\left(\frac{I_1}{A_1}\frac{\partial^6 u_1}{\partial x^4\partial t^2}-\frac{\partial^4 u_1}{\partial x^2\partial t^2}-\frac{\rho I_1}{GA_1\kappa}\frac{\partial^6 u_1}{\partial x^2\partial t^4}+\frac{c}{\rho A_1}\left(\frac{\partial^2 u_2}{\partial x^2}-\frac{\partial^2 u_1}{\partial x^2}\right)+\frac{c}{GA_1\kappa}\frac{\rho I_1}{\rho A_1}\left(\frac{\partial^4 u_2}{\partial x^2\partial t^2}-\frac{\partial^4 u_1}{\partial x^2\partial t^2}\right)\right)\\&=0\end{aligned} \tag{20a}$$

$$\frac{EI_2}{\rho A_2}\frac{\partial^4 u_2}{\partial x^4}-\frac{I_2}{A_2}\left(1+\frac{E}{G\kappa}\right)\frac{\partial^4 u_2}{\partial x^2\partial t^2}+\frac{\partial^2 u_2}{\partial x^2}+\frac{\rho I_2}{GA_2\kappa}\frac{\partial^4 u_2}{\partial t^4}$$
$$+\frac{c}{GA_2\kappa}\left(-\frac{GA_2\kappa}{\rho A_2}(u_1-u_2)+\frac{EI_2}{\rho A_2}\left(\frac{\partial^2 u_1}{\partial x^2}-\frac{\partial^2 u_2}{\partial x^2}\right)-\frac{\rho I_2}{\rho A_2}\left(\frac{\partial^2 u_1}{\partial t^2}-\frac{\partial^2 u_2}{\partial t^2}\right)\right)$$
$$+(e_0a)^2\left(\frac{I_2}{A_2}\frac{\partial^6 u_2}{\partial x^4\partial t^2}-\frac{\partial^4 u_2}{\partial x^2\partial t^2}-\frac{\rho I_2}{GA_2\kappa}\frac{\partial^6 u_2}{\partial x^2\partial t^4}+\frac{c}{\rho A_2}\left(\frac{\partial^2 u_1}{\partial x^2}-\frac{\partial^2 u_2}{\partial x^2}\right)+\frac{c}{GA_2\kappa}\frac{\rho I_2}{\rho A_2}\left(\frac{\partial^4 u_1}{\partial x^2\partial t^2}-\frac{\partial^4 u_2}{\partial x^2\partial t^2}\right)\right)$$
$$=0 \tag{20b}$$

Substitution of Eqs. (12a,b) into Eqs. (20a) and (20b) yields the following equation in matrix form:

$$\begin{bmatrix}\Delta_1 & \Delta_2\\ \Delta_3 & \Delta_4\end{bmatrix}\begin{Bmatrix}U_1\\ U_2\end{Bmatrix}=\begin{Bmatrix}0\\ 0\end{Bmatrix} \tag{21}$$

where

$$\Delta_1=\frac{EI_1}{\rho A_1}k^4-\frac{I_1}{A_1}\left(1+\frac{E}{G\kappa}\right)k^2\omega^2\left(1+\frac{(e_0a)^2k^2}{1+E/G\kappa}\right)-\omega^2(1+(e_0a)^2k^2)+\frac{\rho I_1}{GA_1\kappa}\omega^4(1+(e_0a)^2k^2)$$
$$+\frac{c}{\rho A_1}(1+(e_0a)^2k^2)+\frac{c}{GA_1\kappa}\frac{EI_1}{\rho A_1}k^2-\frac{c}{GA_1\kappa}\frac{\rho I_1}{\rho A_1}\omega^2(1+(e_0a)^2k^2)$$
$$\Delta_2=-\frac{c}{\rho A_1}(1+(e_0a)^2k^2)-\frac{c}{GA_1\kappa}\frac{EI_1}{\rho A_1}k^2+\frac{c}{GA_1\kappa}\frac{\rho I_1}{\rho A_1}\omega^2(1+(e_0a)^2k^2)$$
$$\Delta_3=-\frac{c}{\rho A_2}(1+(e_0a)^2k^2)-\frac{c}{GA_2\kappa}\frac{EI_2}{\rho A_2}k^2+\frac{c}{GA_2\kappa}\frac{\rho I_2}{\rho A_2}\omega^2(1+(e_0a)^2k^2)$$
$$\Delta_4=\frac{EI_2}{\rho A_2}k^4-\frac{I_2}{A_2}\left(1+\frac{E}{G\kappa}\right)k^2\omega^2\left(1+\frac{(e_0a)^2k^2}{1+E/G\kappa}\right)-\omega^2(1+(e_0a)^2k^2)+\frac{\rho I_2}{GA_2\kappa}\omega^4(1+(e_0a)^2k^2)$$
$$+\frac{c}{\rho A_2}(1+(e_0a)^2k^2)+\frac{c}{GA_2\kappa}\frac{EI_2}{\rho A_2}k^2-\frac{c}{GA_2\kappa}\frac{\rho I_2}{\rho A_2}\omega^2(1+(e_0a)^2k^2)$$

The wave solution can therefore be derived from an eigen-value problem to find non-trivial solutions for U_i ($i=1,2$) in Eq. (21) which is given as

$$\Delta_1\Delta_4-\Delta_2\Delta_3=0 \tag{22}$$

Three cut-off frequencies for the DWNT by both local and nonlocal Timoshenko beam models are thus derived:

$$\omega_{c1}^2=\frac{GA_1\kappa}{\rho I_1},\quad \omega_{c2}^2=\frac{GA_2\kappa}{\rho I_2},\quad \omega_{c3}^2=c\left(\frac{1}{\rho A_1}+\frac{1}{\rho A_2}\right) \tag{23a–c}$$

It can be found that the third cut-off frequency of DWNT via the nonlocal Timoshenko beam model is exactly the same with the sole cut-off frequency for DWNT via the nonlocal Euler–Bernoulli beam model shown in Eq. (16).

Two asymptotic phase velocities at $k\to\infty$ are derived as follows via the local or classical Timoshenko beam model:

$$v_{TL1}=\sqrt{\frac{G\kappa}{\rho}} \tag{24a}$$

$$v_{TL2}=\sqrt{\frac{E}{\rho}} \tag{24b}$$

By comparing the two asymptotic velocities with those in Eqs. (17a) and (17b), it can be concluded that wave solution for the DWNT via the nonlocal Euler–Bernoulli beam model is equivalent to that via the local Timoshenko beam model if the scale coefficient is set $e_0a = 2\sqrt{\kappa + \kappa v}d_1$ to accommodate the first phase wave velocity, or $e_0a = 2\sqrt{2}d_2$ to accommodate the second phase wave velocity, where d_1 and d_2 are mid-surface diameters for inner and outer tubes separately.

One asymptotic phase velocity via the nonlocal Timoshenko beam model is observed from calculations in Eq. (22) and is shown below:

$$v_{\mathrm{TNL}} = \sqrt{\frac{G\kappa}{\rho}} \tag{25}$$

This solution indicates that only one asymptotic velocity is expected to be observed for DWNT in future studies.

Another characteristic to be emphasized is the asymptotic frequency of the DWNT derived as

$$\bar{\omega}_{nT} = \frac{1}{e_0a}\sqrt{\frac{Et}{\rho t}} = \frac{1}{e_0a}\sqrt{\frac{C}{\rho t}} \tag{26}$$

where the in-plane stiffness is $Et = 360\ \mathrm{J/m^2}$ (Yakobson et al., 1996) which is a virtually constant parameter. This asymptotic frequency can thus be calculated as $\bar{\omega}_{nT} = \frac{21456}{e_0a}$ if the mass density $\rho = 2.3\ \mathrm{g/cm^3}$ and the thickness of CNT $t = 0.34$ nm are chosen (Yoon et al., 2004). It is easily proven that the value is also valid for a SWNT.

As indicated, parameter a describes internal characteristic length, and it was chosen as the length of a C–C bond, which is 0.142 nm, for analysis of CNTs (Sudak, 2003). On the other hand, the parameter e_0 was given as 0.39 (Eringen, 1983). This value has to be determined from experiments by matching dispersion curves of plane waves. But this has not yet been achieved for CNTs. It was speculated (Peddieson et al., 2003) that the value might even be a value on the order of hundreds. Based on Eq. (26), a rough estimate of the scale coefficient e_0a becomes possible as long as the highest frequency of a SWNT or a DWNT can be available since vibration of a bounded medium can be seen as a standing wave phenomenon in the medium. An available experimental work on the vibration of CNTs in reference (Krishnan et al., 1998) provides the fundamental frequency is around 0.1 THz. If this value is substituted in Eq. (26), it can be derived that $e_0a < 210$ nm. As stated in references (Yoon et al., 2004), the frequency in CNTs is in the terahertz range. A conservative evaluation on the scale coefficient can be obtained as $e_0a < 2.1$ nm if the maximum frequency value for a known SWNT or a DWNT is assessed to be greater than 10 THz. It is note that the coefficient is a diameter-dependent variable.

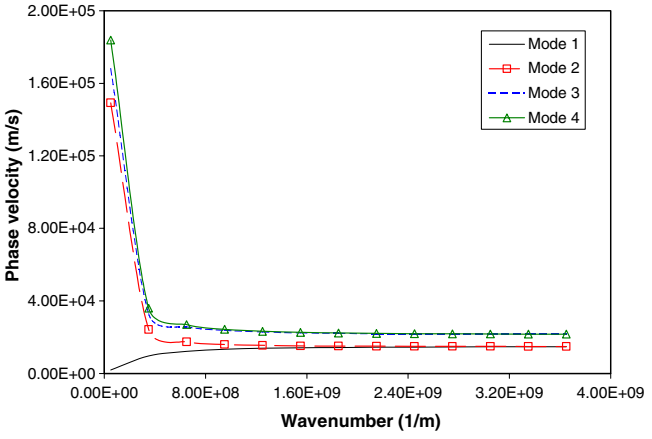

Fig. 3a. Dispersive curves from Timoshenko beam model at $e_0a = 0$ nm.

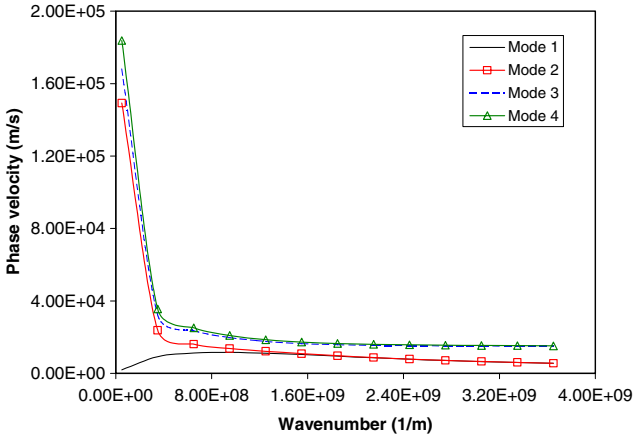

Fig. 3b. Dispersive curves from Timoshenko beam model at $e_0a = 1$ nm.

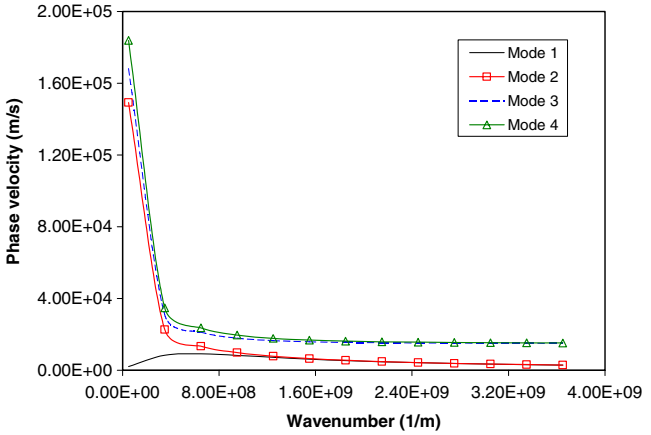

Fig. 3c. Dispersive curves from Timoshenko beam model at $e_0a = 2$ nm.

Dispersion curves for the DWNT with the inner diameter $d_1 = 5$ nm are plotted in Figs. 3a–3c at $e_0a = 0$ nm, $e_0a = 1$ nm, and $e_0a = 2$ nm respectively. First observation verifies the conclusions from Eqs. (24a), (24b) and (25) that there are two asymptotic phase velocities from the LOCAL Timoshenko beam model shown in Fig. 3a, whereas there is only one asymptotic velocity via the NONLOCAL Timoshenko beam model shown both in Figs. 3b and 3c. In Fig. 3a, the phase velocities for the first and second modes converge to the asymptotic value given in Eq. (24a), while the velocities for the third and the fourth modes converge to the asymptotic value given in Eq. (24b). However, when the nonlocal continuum model is applied, it is seen that the velocities for the first and the second modes decrease with increase of wavenumbers seen from Figs. 3b and 3c. However, the velocities for the third and fourth mode of wave come to the asymptotic value as shown in Eq. (25). In addition, from all the three figures, it is found that all the velocities from the three higher modes of wave propagation of the DWNT decrease from higher values at small wavenumbers.

The phase velocity of the DWNT with $d_1 = 5$ nm versus the scale coefficient e_0a via the nonlocal Timoshenko beam model is plotted in Figs. 4a–4c at $k = 5 \times 10^8$/m, $k = 1 \times 10^9$/m, and $k = 5 \times 10^9$/m respectively. First observation is that the scale effect is almost invisible at smaller wavenumbers, such as $k = 5 \times 10^8$/m in Fig. 4a. However, the scale effect becomes more obvious in Fig. 4b and 4c from which it is seen the phase velocities for all the four modes decrease with increase of the scale coefficient. However, this decreasing variation for the third and fourth mode end at larger wavenumbers such as $k = 5 \times 10^9$/m seen in Fig. 4c, whereas, velocities for the first and the second modes decrease to zero as discussed in Figs. 3b and 3c previously.

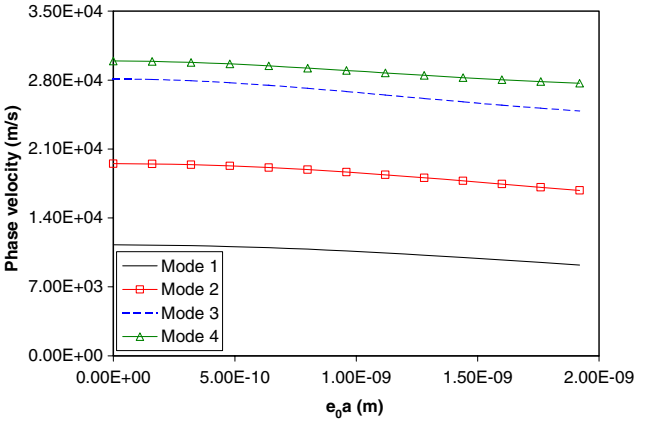

Fig. 4a. Dispersive curves from Timoshenko beam model at $k = 5 \times 10^8$ m^{-1}.

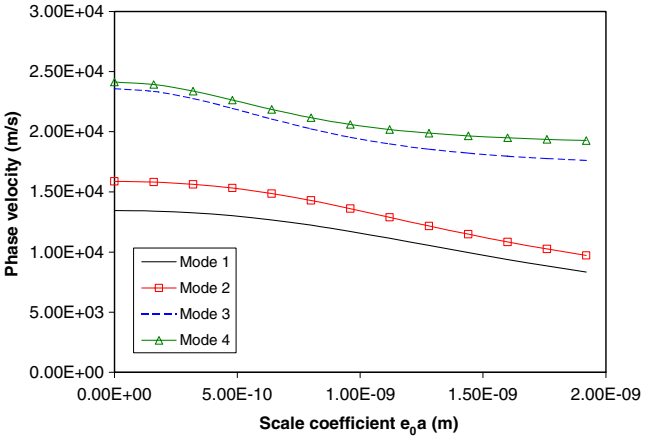

Fig. 4b. Dispersive curves from Timoshenko beam model at $k = 1 \times 10^9$ m^{-1}.

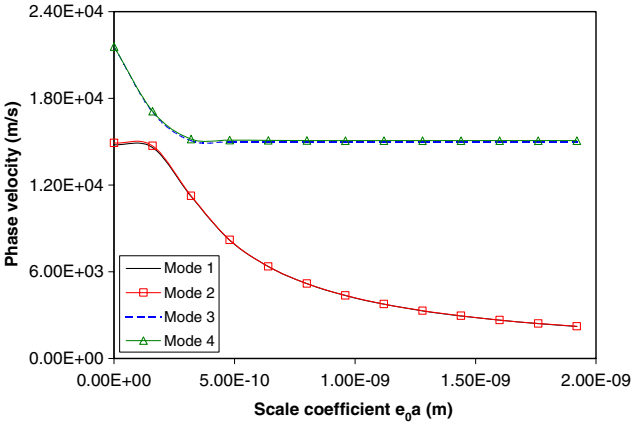

Fig. 4c. Dispersive curves from Timoshenko beam model at $k = 5 \times 10^9$ m^{-1}.

In Figs. 5a–5c, the scale effect on the phase velocities versus the inner diameter of the DWNT at $e_0a = 2$ nm is studied at different wavenumbers $k = 5 \times 10^8$/m, $k = 1 \times 10^9$/m, and $k = 5 \times 10^9$/m respectively. It is seen

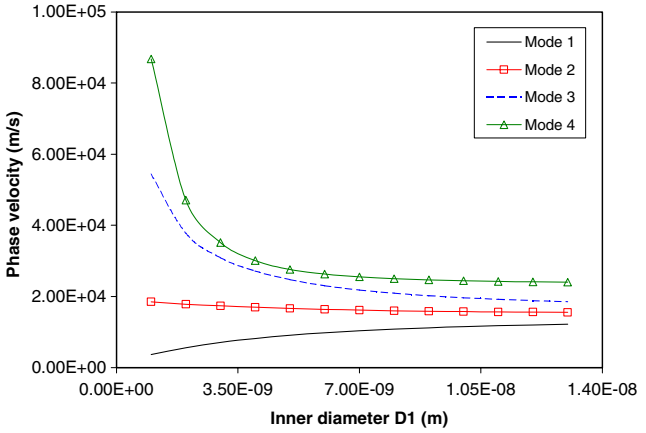

Fig. 5a. Dispersive curves from at $k = 5 \times 10^8\ \mathrm{m}^{-1}$ and $e_0a = 2$ nm.

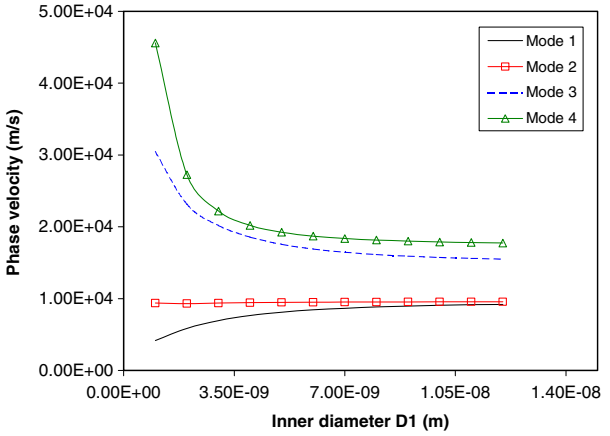

Fig. 5b. Dispersive curves from at $k = 1 \times 10^9\ \mathrm{m}^{-1}$ and $e_0a = 2$ nm.

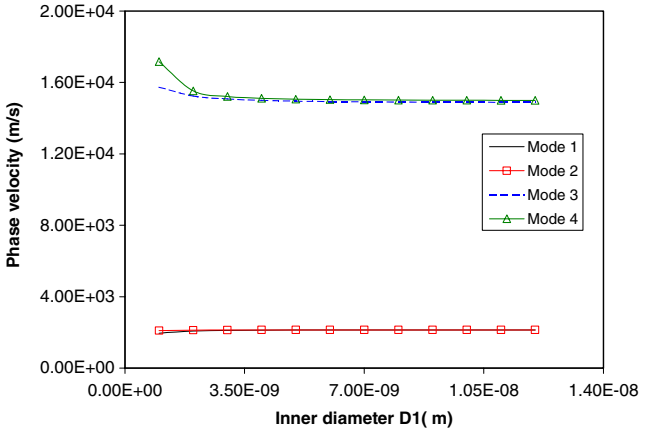

Fig. 5c. Dispersive curves from at $k = 5 \times 10^9\ \mathrm{m}^{-1}$ and $e_0a = 2$ nm.

that at the lower wavenumber $k = 5 \times 10^8$/m in Fig. 5a the velocity for the first mode increase with increase of the diameter, whereas, the velocities for the third and fourth modes decrease with increase of the diameter. Such variation becomes more obvious when the wavenumber arrives at $k = 1 \times 10^9$/m in Fig. 5b. However, when wavenumber increases further to $k = 5 \times 10^9$/m seen in Fig. 5c, the diameter-dependence of the velocities becomes almost invisible. In all the three figures, the velocity for the second mode is relatively insensitive to the diameter compared to those for other modes. The diameter-dependence of wave solution for CNTs is first observed in the manuscript as all previous studies (Sudak, 2003; Zhang et al., 2004) indicated the diameter independent buckling solution of CNTs via nonlocal continuum models.

4. Conclusions

The scale effect on DWNT's wave propagation is studied in the research via the nonlocal continuum beam models. Two-mode solutions and four-mode solutions are obtained via the nonlocal Euler–Bernoulli and Timoshenko beam models respectively. It is shown that the solution via the nonlocal Euler–Bernoulli beam model is equivalent to that via the local Timoshenko beam model if the scale coefficient is adjusted accordingly. The results of dispersion velocities via the nonlocal Timoshenko beam model show that one asymptotic velocity exists. The scale effect becomes more obvious with increase of the scale coefficient for four modes, but tends to invisible for the third and fourth modes at higher wavenumbers. It is also concluded that at lower wavenumbers the velocity for the first mode increase with increase of the diameter, whereas, the velocities for the third and fourth modes decrease with increase of the diameter. However, when wavenumber becomes very high, the dependence of the velocities becomes almost invisible. In addition, the velocity for the second mode is relatively insensitive to the diameter compared to those for other modes. A rough estimation on the scale coefficient used in the nonlocal continuum mechanics is proposed for CNT analysis the first time in the manuscript.

Acknowledgement

We would like to thank the anonymous reviewers of our manuscript for pointing out the recent publications by Wang and Hu (2005) and Zhang et al. (2005) on a similar subject. Wang and Hu (2005) studied wave propagation of *single-walled CNTs* with two beam models, while Zhang et al. (2005) discussed *vibration* of double-walled CNTs with *Euler–Bernoulli beam model only*. These works were published at about the same time our manuscript was submitted for publication in the International Journal of Solids and Structures but we are pleased to point them out as alternate references to this subject for researchers in the field.

References

Ajayan, P.M., Zhou, O.Z., 2001. Application of carbon nanotubes. Topics in Applied Physics 80, 391–425.

Antonelli, G.A., Maris, H.J., 2002. Picosecond ultrasonics study of the vibrational modes of a nanostructure. Journal of Applied Physics 91, 3261–3267.

Ball, P., 2001. Roll up for the revolution. Nature (London) 414, 142–144.

Baughman, R.H., Zakhidov, A.A., de Heer, W.A., 2002. Carbon nanotubes—the route toward applications. Science 297, 787–792.

Brauns, E.B. et al., 2002. Complex local dynamics in DNA on the picosecond and nanosecond time scales. Physical Review Letters 88, 158101-1–158101-4.

Eringen, A.C., 1976. Nonlocal Polar Field Models. Academic, New York.

Eringen, A.C., 1983. On differential equations of nonlocal elasticity and solutions of screw dislocation and surface waves. Journal of Applied Physics 54, 4703–4710.

Hernandez, E., Goze, C., Bernier, P., Rubio, A., 1998. Elastic properties of C and BxCyNz composite nanotubes. Physical Review 80, 4502–4505.

Iijima, S., Brabec, C., Maiti, A., Bernholc, 1996. Structural flexibility of carbon nanotubes. Journal of Chemical Physics 104, 2089–2092.

Jeon, T., Kim, K., 2002. Terahertz conductivity of anisotropic single walled carbon nanotube films. Applied Physics Letters 80, 3403–3405.

Krishnan, A., Dujardin, E., Ebbesen, T., Yianilos, P.N., Treacy, M.M.J., 1998. Young's modulus of singled-walled nanotubes. Physical Review B 58, 14043–14049.

Lau, K.T., 2003. Interfacial bonding characteristics of nanotube/polymer composites. Chemical Physics Letters 370, 399–405.

Peddieson, J., Buchanan, G.R., McNitt, R.P., 2003. Application of nonlocal continuum models to nanotechnology. International Journal of Engineering Science 41, 305–312.

Ru, C.Q., 2000a. Effective bending stiffness of carbon nanotubes. Physical Review B 62, 9973–9976.
Ru, C.Q., 2000b. Elastic bucking of singled-walled carbon nanotubes ropes under high pressure. Physical Review B 62, 10405–10408.
Sanchez-Portal, D. et al., 1999. Ab initio structural, elastic, and vibrational properties of carbon nanotubes. Physical Review B59, 12678–12688.
Sharma, P., Ganti, S., Bhate, N., 2003. Effect of surfaces on the size-dependent elastic state of nano-inhomogeneities. Applied Physics Letters 82, 535–537.
Sheehan, P.E., Lieber, C.M., 1996. Nanotribology and nanofabrication of MoO_3 structures by atomic force microscopy. Science 272, 1158–1161.
Sirtori, C., 2002. Applied physics: bridge for the terahertz gap. Nature (London) 417, 132–133.
Sudak, L.J., 2003. Column buckling of multiwalled carbon nanotubes using nonlocal continuum mechanics. Journal of Applied Physics 94, 7281–7287.
Timoshenko, S.P., 1921. On the correction for shear of the differential equation for transverse vibrations of prismatic bars. Philosophical Magazine 41, 744–746.
Wang, L.F., Hu, H., 2005. Flexural wave propagation in single-walled carbon nanotubes. Physical Review B 71, 195412.
Wang, Q., 2004. Effective in-plane stiffness and bending rigidity of armchair and zigzag carbon nanotubes. International Journal of Solids and Structures 41, 5451–5461.
Wang, Q., Hu, T., Chen, G., Jiang, Q., 2005. Bending instability characteristics of double-walled carbon nanotubes. Physical Review B 71, 045403-1–045403-8.
Wang, Q., Varadan, V.K., 2005. Stability analysis of carbon nanotubes via continuum models. Smart Materials and Structures 14, 281–286.
Yakobson, B.I., Brabec, C.J., Bernholc, J., 1996. Nanomechanics of carbon tubes: instabilities beyond linear range. Physical Review Letters 76, 2511–2514.
Yakobson, B.I., Smalley, R., 1997. Fullerene nanotubes: C1,000,000 and beyond. American Scientist 85, 324–327.
Yakobson, B.I., Campbell, M.P., Brabec, C.J., Bernholc, J., 1997. High strain rate fracture and C-chain unraveling in carbon nanotubes. Computational Materials Science 8, 241–248.
Yoon, J., Ru, C.Q., Mioduchowski, A., 2003. Sound wave propagation in multiwall carbon nanotubes. Journal of Applied Physics 93, 4801–4806.
Yoon, J., Ru, C.Q., Mioduchowski, A., 2004. Timoshenko-beam effects on transverse wave propagation in carbon nanotubes. Composites Part B: Engineering 35, 87–93.
Zhang, Y.Q., Liu, G.R., Wang, J.S., 2004. Small-scale effects on buckling of multiwalled carbon nanotubes under axial compression. Physical Review B 70, 205430-1–205430-6.
Zhang, Y.Q., Liu, G.R., Xie, X.Y., 2005. Free transverse vibrations of double-walled carbon nanotubes using a theory of nonlocal elasticity. Physical Review B 71, 195404.